European Journal of Orthodontics, 2021, 1–8
doi:10.1093/ejo/cjab034
Original article

Original article

Facial asymmetry assessment in skeletal Class III patients with spatially-dense geometric morphometrics

Yi Fan[1,2,3,*], Wei He[4,*], Gui Chen[1,2], Guangying Song[1,2], Harold Matthews[3,5,6], Peter Claes[3,5,6,7], Ruoping Jiang[1,2] and Tianmin Xu[1,2]

[1]Department of Orthodontics, Peking University School and Hospital of Stomatology, Beijing, China, [2]National Engineering Laboratory for Digital and Material Technology of Stomatology, Beijing Key Laboratory of Digital Stomatology, Peking University School and Hospital of Stomatology, Beijing, China, [3]Facial Science, Murdoch Children's Research Institute, Melbourne, Australia, [4]Department of Oral and Maxillofacial Surgery, Peking University School and Hospital of Stomatology, Beijing, China, [5]Department of Human Genetics, KU Leuven, Leuven, Belgium, [6]Medical Imaging Research Center, University Hospitals Leuven, Leuven, Belgium, [7]Department of Electrical Engineering, ESAT/PSI, KU Leuven, Leuven, Belgium

*Yi Fan and Wei He equally contributed to this work and are co-first authors.

Correspondence to: Tianmin Xu, Department of Orthodontics, Peking University School and Hospital of Stomatology, No.22, Zhongguancun South Avenue Haidian District, Beijing, 100081, China. E-mail: tmxuortho@163.com

Summary

Objective: Quantification and visualization of the location and magnitude of facial asymmetry is important for diagnosis and treatment planning. The objective of this study was to analyze the asymmetric features of the face for skeletal Class III patients using spatially-dense geometric morphometrics.

Methods: Three-dimensional facial images were obtained for 86 skeletal Class III patients. About 7160 uniformly sampled quasi-landmarks were automatically identified on each face using template mapping technique. The pointwise surface-to-surface distance between original and mirror face was measured and visualized for the whole face after robust Procrustes superimposition. The degree of overall asymmetry in an individual was scored using a root-mean-squared-error. Automatic partitioning of the face was obtained, and the severity of the asymmetry compared among seven facial regions.

Results: Facial asymmetry was mainly located on, but not limited to, the lower two-thirds of the face in skeletal Class III patients. The lower cheek and nose asymmetry were detected to have more extensive and of a greater magnitude of asymmetry than other facial anatomical regions but with various individual variations. The overall facial asymmetry index and the regional facial asymmetry indices were higher in males and patients with chin deviation.

Conclusions: Soft tissue asymmetry is predominately presented in the lower-third of the face in skeletal Class III patients and with various variations on other facial anatomical regions. Morphometric techniques and computer intensive analysis have allowed sophisticated quantification and visualization of the pointwise asymmetry on the full face.

Introduction

Facial asymmetry is frequently observed in patients with skeletal Class III deformity (1). Severe and progressive asymmetry is highly visible and is often one of the patient's major complaints. As a patient's perception of the need for orthognathic surgery is strongly influenced by the preoperative severity of the facial asymmetry and a patient's satisfaction with the outcomes is strongly influenced by the postoperative asymmetry correction; an accurate and objective analysis of the location and magnitude of facial asymmetry is important for diagnosis, treatment planning, evaluation of treatment outcomes as well as to assist with patient communication in determining etiology (2, 3).

Several approaches for calculating facial asymmetry have been presented in the past. The main approach in the orthodontic literature is to divide the face into left and right hemifaces. A reference midline is often generated by connecting median landmarks or bisecting the interval between bilateral landmarks of the midface. Differences between paired bilaterally corresponding linear distances, angles, areas or ratios measurements, taken perpendicularly to the reference midline, are compared (4, 5). However, conventional measurements often fail to represent the complete face. Asymmetry of the facial regions such as the cheek and chin, where traditional landmarks are sparse or poorly defined, cannot be quantified comprehensively with these conventional measurements.

Recently, more spatially complete forms of asymmetry analysis grounded in Geometric morphometric is advised in the literature (6, 7). Geometric morphometrics, which is the multivariate statistical analysis of shape and form, offer a suite of mathematical and statistical tools to treat 3D structures in a much more sophisticated way (8, 9). Klingenberg et al. firstly assessed asymmetry by comparing corresponding landmarks between the original image and its reflection (10). If a face is perfectly symmetrical, the designated landmarks on the original structure and its mirror structure could be superimposed precisely. If not, the discrepancy between the two indicates where the asymmetry occurred. Claes et al. further extended the Klingenberg protocol by indicating a dense set of landmarks across the face with an automated computer algorithm (11). Then the dense landmarks on the original face and its reflection are compared (12). This offers a methodologically superior approach to evaluate asymmetry of the entire face. In addition, the asymmetry could be visualized pointwise on the face, which provides direct and intuitive feedback to clinicians and patients.

In this study, we aimed, with the use of spatially-dense geometric morphometric technique, to quantify and visualize the facial asymmetry for skeletal Class III patients in 3D. We also compare the severity of asymmetry in different facial anatomical regions.

Materials and methods

Patients

We screened patients who required surgical-orthodontic treatment to correct dentofacial deformity at Peking University School and Hospital of Stomatology, Beijing, China, from 2015–18. The sample selection was performed as follows: 1. Adults patients: males >18 years of age, females >16 years of age; 2. Skeletal Class III malocclusion: ANB < 0°, Wits <4mm; Patients who had syndromes or congenital anomalies, history of maxillofacial trauma or with a history of previous surgical treatment. The study was approved by the Institutional Review Board of the Peking University School and Hospital of Stomatology (PKUSSIRB-202057109). All participants provided written informed consent before participation.

Facial imaging acquisition

Each subject had a pretreatment 3D photograph captured using the 3dMD imaging system (3dMD Inc, Atlanta, GA) and was stored in an obj file. This records each face as a cloud of 3D point co-ordinates, interconnected to define the facial surface. The patients were instructed to maintain a neutral facial expression in their natural head position when scanned, with lips and mouth at rest and teeth in intercuspation to minimize involuntary movement (13).

Automatic quasi-landmark identification

An automated template mapping strategy was used to standardize the 3D facial images (14). The aim is to automatically identify the same set of dense points on each image. Briefly, a generic template face, represented by 7160 quasi-landmarks, was translated, rotated and scaled (rigid registration) to roughly align to each target face. Then the template was deformed (non-rigid registration) to fit precisely on each the target face (Figure 1). Applying this to each original and mirror image (created by reversing the sign of the x-coordinate of each point on the original) allows the superimposition and comparison of bilaterally corresponding points between original and mirror images. The mid-sagittal plane was fitted through the midpoints between each corresponding point on the original quasi-landmark configuration and the mirrored and aligned quasi-landmark configuration (11). An open-source implementation of the template mapping algorithm is available at https://github.com/TheWebMonks/meshmonk (14). After the template mapping, this resulted in 7160 quasi-landmarks that capture the entire facial region while automatically removing irrelevant structures such as hair, ears, shoulders, and any irrelevant polygons.

Facial asymmetry evaluation

Overall facial asymmetry

The robust Procrustes superimposition was applied to superimpose the original face and the mirror face (11, 12). The distance at each point (in mm) between each original and mirror face was visualized on the original configuration as a color map. This reflects the location and magnitude of asymmetry found in an individual (Figure 2). An overall asymmetry index was obtained by calculating the root mean square of the distances (errors; RMSE) between the superimposed landmarks of the original and mirror configurations (11, 15).

Automatic partitioning of the face and asymmetry evaluation of different facial regions

The template face was partitioned into seven anatomical regions. The method used by Duran et al. (16) was modified for the segmentation of the face. The landmarks that were used to partition the face were in Table 1. Two independent observers placed landmarks twice on the template face, with one week between landmarking sessions, resulting in four sets of facial anatomical landmark indications for the template. The average of the four sets of indications represented the final manual landmarks on the template.

The planes that were used to obtain soft tissue regions were as follows:

(1) Mid-sagittal plane: the mid-sagittal plane was firstly generated by construction of the midpoint of the face (11).
(2) Orbital plane: the plane passing through left and right orbita (Or) point and perpendicular to the mid-sagittal plane;

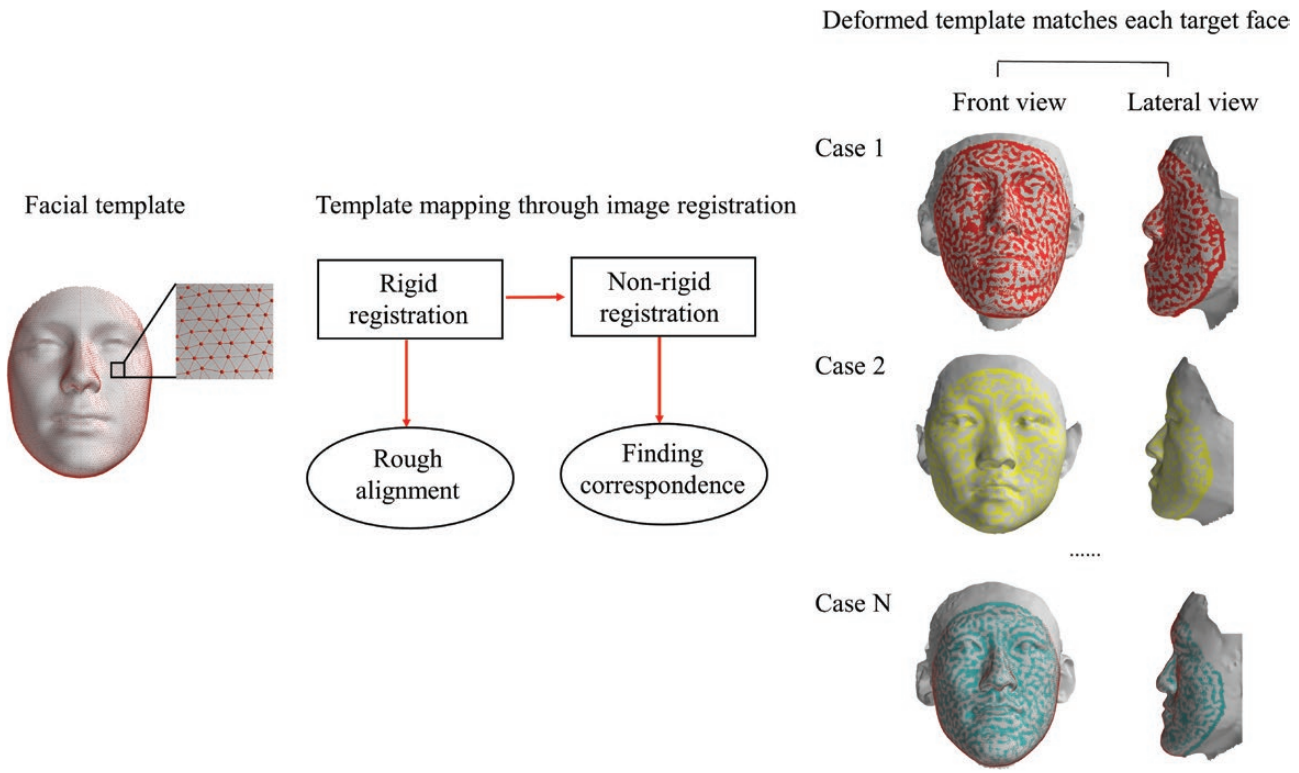

Figure 1. Workflow for the template mapping technique.

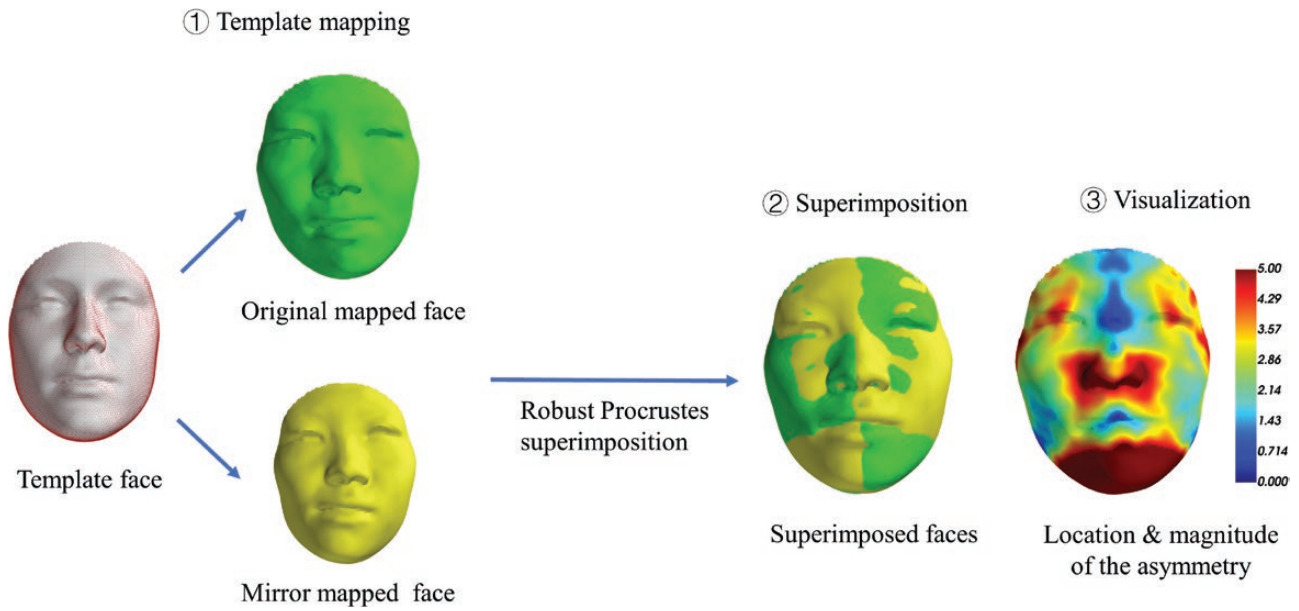

Figure 2. Diagram of facial asymmetry assessment. (1) Establishing correspondence between the original and mirror face via template mapping. (2) Aligning the original mapped face and the mirror mapped face through robust Procrustes superimposition. (3) Visualization of the superimposed faces: the difference at each point on the original mapped face and the mirror mapped face is visualized on the original configuration as color map.

(3) Glabella plane: the plane parallel to the orbital plane and passing through soft-tissue glabella (G);
(4) Subnasal plane: the plane parallel to the orbital plane and passing through the subnasale (Sn) point;
(5) Mouth plane: the plane parallel to the orbital plane and passes through the left and right commissure (Com) points;
(6) Lower lip plane: the plane parallel to the orbital plane and passing through the sublingual (Sl) point;
(7) Cheek plane: the plane passes through the Endocanthion (En) and Comissure (Com) point.

Seven anatomical regions: nose (nose bridge, tip and alare), upper lip, lower lip, upper cheek, and lower cheek and chin were obtained on the template (Figure 3).

Because the registered faces are represented by the same points as the template, the manually defined facial patches could be subsequently transferred from the template to each subject as they

Table 1. Description of landmarks for partition of the face.

Landmark	Abbreviation	Definition
Glabella	G	Most prominent midline point between eyebrows
Endocanthion	En	Point at the inner commissure of the eye fissure
Soft tissue orbitale	Or	Most inferior point of infraorbital rim
Sub-nasale	Sn	Most retruded point in the concavity between nose and upper lip
Comissure	Com	Point at labial commissure
Sublabiale	Sl	Deepest midpoint on the labiomental soft tissue contour

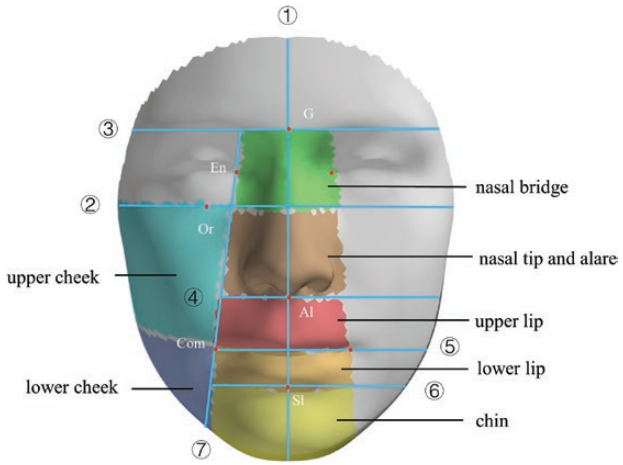

Figure 3. Partition of the face into seven facial regions. The planes that were used to obtain soft tissue regions: (1) Mid-sagittal plane; (2) Orbital plane; (3) Glabella plane; (4) Subnasal plane; (5) Mouth plane; (6) Lower lip plane; (7) Cheek plane.

were represented by the same correspondence, thus automatically performing facial partition on each patient. The asymmetry index (RMSE) of different regions were calculated. Boxplots for the asymmetry index for different facial regions were obtained.

Sexual dimorphism of the facial asymmetry

The overall facial asymmetry index and regional asymmetric indices were compared between males and females in skeletal Class III patients.

Facial asymmetry comparison between the chin deviated group and non-deviated group

The subjects were further subdivided according to the degree of the soft tissue Menton (Me') deviation from the midsagittal plane. In general, skeletal deviation must be equal to or greater than 2–4 mm in order to render the asymmetry visible in an individual's face (17). Nevertheless, facial asymmetry is usually less severe due to soft tissue compensation. For this reason, patients with 2 mm or more of 2 mm Me' deviation from the midsagittal plane were categorized as chin deviated group in this study, whereas patients with less than 2 mm of Me' deviation comprised the non-chin deviated group.

The Me' was automatically identified on each facial image to ensure the precision and reproducibility. Two independent observers (an experienced orthodontist and an experienced maxillofacial surgeon) determined the protocol for placing Me' on the 3D photo. They placed Me' twice each with an interval of 48-hour on the template face, resulting in four Me' indications. The average Me' coordinate was used as the final manual landmark indication on the template. Then, the Me' was automatically transferred onto each Class III face following a barycentric to Cartesian coordinates (x,y,z co-ordinates) conversion as described in previous publications (14, 18). Because the landmark indication procedure was automatic, thus it is highly reproducible. The accuracy of the automatic landmark indication was compared to manual landmark indication of Me' annotated on 20 random selected faces. The mean of three intraclass correlation coefficients (ICC), one for each of the x-, y- and z-coordinates between manual and automatic landmark indications was 0.993, 0.997 and 0.997 respectively.

The overall facial asymmetry index and regional asymmetric indices were compared between patients with and without chin deviation. All the analyses were performed using custom-written code in the Python programming language.

Statistical analysis

Descriptive statistics (means and standard deviations) were computed for age and cephalometric measurements. Histograms and skewness test were used to check the normality of the facial asymmetry parameters. The overall facial asymmetry index and regional indices followed positively skewed distribution. Therefore, Mann–Whitney *U*-test was used for gender comparison and chin deviated/non deviated groups comparison via IBM SPSS statistical software (version 23.0; IBM, Armonk, NY). At $P < 0.05$, the difference was considered significant.

Results

Thirty males and 56 females with skeletal Class III malocclusion and with an overall mean age 20.30 ± 3.78 years were included. The ANB was –3.72 ± 2.15 (mean ± SD) and the Wits appraisal was –10.33 ± 3.36 (mean ± SD).

Overall facial asymmetry

Nine individuals were selected to illustrate the color-maps visualization effects of the facial asymmetry (Figure 4). Red areas indicate regions where the asymmetry was larger than 4 mm and dark blue areas indicate no asymmetry. The results indicated that the facial asymmetry varied from none to considerable. Pronounced asymmetry was frequently observed in the chin, the cheek and the nasal and paranasal regions. The asymmetry index (AI) indicated the overall severity of the facial asymmetry for each patient.

Automatic partition of the face and facial regions asymmetry evaluation

According to the box plots, the highest median asymmetry index was observed in the chin, followed by the lower cheek, lower lip, nasal tip and alare (Figure 5). The chin has the highest median value and the largest range, indicating chin asymmetry had the most individual variation.

Sexual dimorphism of the facial asymmetry

The ANB was –3.54 ± 2.08 (mean ± SD) in male patients and was –3.81 ± 2.20 (mean ± SD) in female patients. The overall facial asymmetry index was statistically higher in males than in females. Regional facial asymmetry indices were also higher in males, but

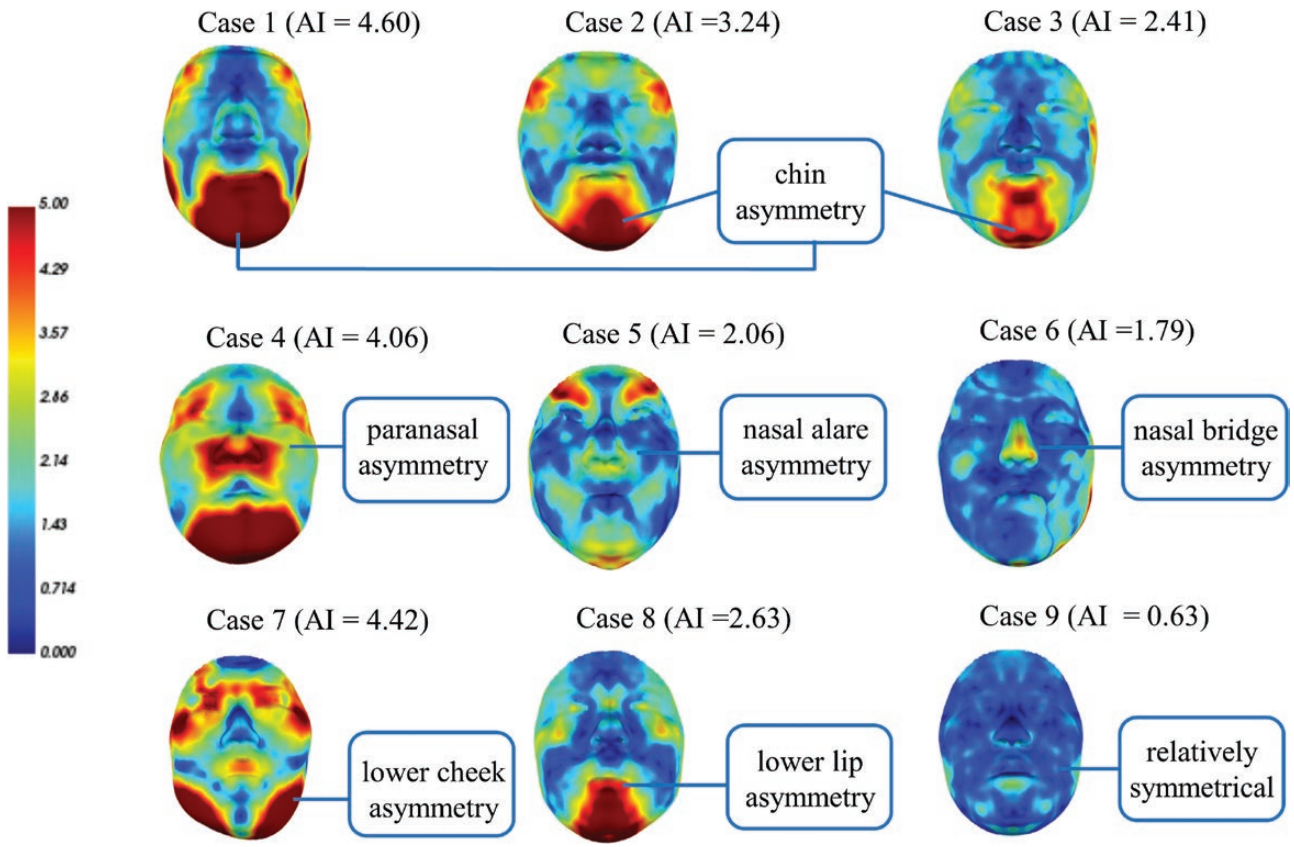

Figure 4. Visualization of facial asymmetry for nine individuals. The colormap indicates the magnitude of the asymmetry at each point on the full face, with red indicating the asymmetry larger than 4mm and dark blue indicating no asymmetry. The first row shows various degrees of the chin asymmetry. The second row shows nasal and paranasal asymmetry. The third row shows lower cheek asymmetry, lip asymmetry, and relative symmetry. The asymmetry index (AI) indicates the severity of the facial asymmetry for each patient.

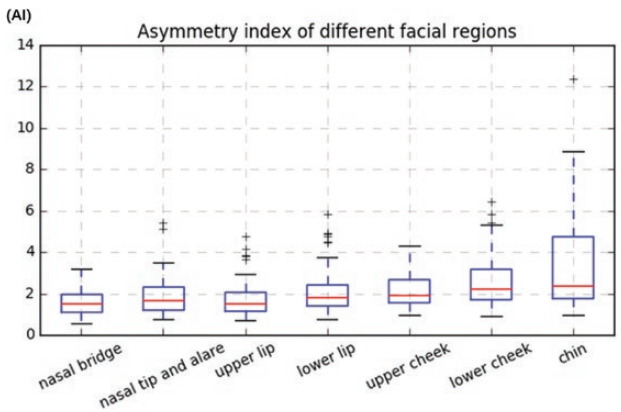

Figure 5. Boxplots of the asymmetry index (AI) of different facial regions. Red lines indicate the median. The limits of the boxes indicate the interquartile range (IQR), whiskers indicate the range of the data up to 1.5 times the IQR from the edge of the box. Outliers outside this range are shown as plus symbols.

only the nasal tip and alare, lower cheek and chin were statistically more asymmetric in males than in females (Table 2).

Facial asymmetry comparison between the chin deviated group and non-deviated group

The differences of the facial asymmetry index between the chin deviated group and the non- deviated group were shown in Supplementary Table 1. Twenty-nine patients (ANB: –3.38 ± 2.01(mean ± SD)) were categorized as having chin deviation and 57 patients (ANB: –3.89 ± 2.22 (mean ± SD)) were categorized as having non- chin deviation in this cohort. There were significant differences in overall facial asymmetry and all the regional asymmetric indices except for the upper lip asymmetry between patients with and without chin deviation.

Discussion

Soft-tissue properties have become important owing to the increasing esthetic concerns of patients seeking orthodontic, combined with orthognathic treatment. We employed a 3D, rapid and automatic asymmetry evaluation method, grounded in spatially-dense geometric morphometrics, to investigated the facial asymmetry in skeletal Class III patients. This technique provides pointwise quantification and visualization of asymmetry of the entire face. We found that soft tissue asymmetry is predominately presented in the lower-third of the face. Cheek and nose asymmetries have also been frequently observed, but with various individual variations. As these asymmetric features will directly relate to the final aesthetic outcome of the patients, diagnosis, and correction the facial asymmetry of the skeletal Class III patient is multifaceted and must be evaluated individually and comprehensively in 3D.

Previous studies, using landmark-based 2D analysis, have indicated that facial asymmetry is predominantly located in the chin in skeletal Class III patients (19). It has been reported that facial asymmetry was observed in 40 % (20) to 80 % (21) adult Class III patients as assessed by extra-oral photographs or X-ray analysis.

Table 2. Sexual dimorphism of the facial asymmetry in skeletal Class III patients. IQR, interquartile range (25th, 75th percentile); AI: asymmetry index.

	Males (n = 30)		Females (n = 56)		
	Median (IQR)	Minimum, maximum		Minimum, maximum	*P*-values
facial AI	2.30(2.01,3.20)	(1.49,4.50)	1.98(1.73,2.63)	(1.09,5.90)	0.035*
nasal bridge AI	1.67(1.24,2.01)	(1.01,3.21)	1.43(1.05,2.00)	(0.58,2.99)	0.145
nasal tip and alare AI	2.01(1.44,2.59)	(1.04,3.46)	1.49(1.12,2.21)	(0.74,5.45)	0.029*
upper lip AI	1.92 (1.38,2.15)	(0.78,4.16)	1.46(1.15,2.07)	(0.71,4.78)	0.250
lower lip AI	1.92 (1.36,2.56)	(0.76,5.82)	1.72(1.41,2.43)	(0.90,4.85)	0.556
upper cheek AI	2.22(1.70,2.65)	(1.06,3.48)	1.83(1.41,2.69)	(0.99,4.33)	0.133
lower cheek AI	2.74(2.15,3.54)	(0.98,5.85)	2.03(1.65,3.13)	(0.91,6.46)	0.046*
chin AI	2.88 (2.10,5.15)	(1.45,8.75)	2.23(1.55,4.16)	(0.99,12.36)	0.046*

Note. Group difference was determined using Mann–Whitney U-test. *$P < .05$.

However, these studies rely on isolated variables such as distances or angles, compared between the two hemifaces, which only provide a sparse representation of the face and are inadequate for assessing and visualizing the complex features of the asymmetry. Moreover, these studies have evaluated facial asymmetry focusing on the lower third of the face, with little exploration of other anatomical regions, especially those regions underrepresented by traditional anatomical landmarks.

Three-dimensional surface imaging provides a powerful tool to accurately capture and preserve the 3D form of the entire face. In this study, the chin was identified as the most asymmetric region and with relatively large individual variation among skeletal Class III patients, which is consistent with previous findings (1, 16). This most likely results from positional displacement or morphological alteration of the mandible (17, 22). Pronounced asymmetry has also been detected in the cheek and nose, which have been rarely investigated in related literature. The asymmetry index in the lower cheek is higher than the upper cheek, this could be due to the "pulling effect" of the deviated chin. In general, the cheek has higher asymmetry indices than other anatomical regions, which may also be related to the shape and function of the masticatory muscles. Goto et al. found that the masseter muscle was significantly shorter and of lower volume on the deviated side and this could reflect the difference in the spatial anatomy (23). As the masticatory muscles are unlikely to be altered by the relocation of the maxilla and the mandible, then the risk of residual asymmetry of the cheek should be advised to patients before the start of the treatment. Nasal and paranasal asymmetry have also been identified. The location and the severity of the asymmetry is pinpointed by the colour map, which enables to locate the asymmetry either on the nasal bridge, tips or alare and from slight to severe asymmetry. As nasal preoperative asymmetric features are also unlikely to be corrected and may continue to affect the perception of the facial aesthetics, therefore, postoperative rhinoplasty could be suggested to these patients if they have a high expectation of the aesthetic outcome. Asymmetry of the lips is characterized as the difference on the two sides of the corners of the mouth or with distorted vermilion borders of the upper and lower lips. The lip anatomically consists of the depressor anguli oris, mentalis and depressor labii inferioris muscles, which have their origins in the mandible and insertion in the cutis of the lower lip. Therefore, deviation of the mandible may change the courses of these muscles, pulling the orbicularis oris and the cutis to the deviated side, and consequently deforming both upper and lower lips (24). The color map-based visualization and quantification provides intuitive representation of the location of the asymmetry, determines the amount of facial asymmetry for diagnostic purposes and improves the understanding of the etiology. This is also important for improving communication and education with the patient, especially where asymmetry is located beyond the scope of orthodontic and orthognathic treatment.

The overall facial asymmetry index and the regional facial asymmetry indices were higher in males than in females. One explanation is that female patients usually pay more attention to facial appearance and are willing to be treated when they become aware of asymmetrical facial features. The overall facial asymmetry index and the regional asymmetry indices were significant higher in the chin deviated group than the non-deviated group. This indicates that in patients for whom asymmetric growth of the mandible occurred, there also occurred some adaptation of other parts of the face. Soft tissue compensation has been detected previously in patients with hemimandibular hyperplasia and hemimandibular elongation anomalies by Walter et al. (15). However, the maxillary process develops separately from the mandibular process and the maxilla is rigidly attached to the stable region of synchondroses at the cranial base. Adaptation of these two structures may occur but is not certain to occur in all cases. Therefore, the clinical correction of asymmetry remains challenging and individualized assessment should be performed to evaluate preexisting asymmetric features before treatment.

From a technological point of view, the most common method of assessing facial asymmetry is the mirror image technique, which is to superimpose the original 3D facial image and its mirror copy. The asymmetry is usually illustrated in a colour map to reflect the disparities between the right and left sides of the face (5, 25, 26). The main drawback of this method is that the registration process of the two corresponding images is usually performed by an Iterative Closest Point (ICP) algorithm, which approximates each point on one surface as its nearest neighbor on the other surface but does not map corresponding points based on anatomical geometry. It has been reported that the closest point correspondence is adequate when the two sides of the structure are not very different (27), but it becomes incorrect when dealing with severely asymmetric cases (2, 28). In this study, we employ an alternative non-rigid template mapping to establish correspondence between the original and mirror facial gestalt. The template mapping also incorporates a closest-point correspondence, but with "closeness" points updated as the template gradually changes its shape, ensuring that anatomically meaningful correspondence is established at the end of the algorithm (2). This was quantitatively assessed by White et al (14). After superimposing the original and mirror face, the accuracy of the correspondences determines the accuracy of the asymmetry assessment as this is based on anatomically meaningful corresponding points.

Three-dimensional photography is widely used in orthodontics and craniomaxillofacial surgery as an accurate and reproducible record of the 3D facial anatomy. It has the potential to be a versatile tool for assessment of the asymmetry and treatment planning. Moreover, fully automatic and objective approach allows for fast and standardized measurements. Big data initiatives are increasingly common in dentistry and surgical disciplines. The computerized automatic asymmetry evaluation approach will be particularly useful for evaluations of large samples. However, as the face only represent the outer envelope of the craniofacial surface and it can be affected by dental, skeletal as well as muscle components, future studies in this area would benefit from incorporating dental and skeletal components by co-registering cone-beam computed tomography to identify the combined soft and hard tissue effect. In addition, it will be also interesting to evaluate and visualize the post-treatment effect of these patients in future studies.

The limitations of the techniques are: first, although the automatic assessment strategy addresses much of the repeat-measurement variation inherent in manual landmark indication, the errors inherent to rigid ICP registration remains. Therefore, at the level of an individual the mapping can still fail, and the accuracy should always be assessed by the user. Second, the Meshmonk toolbox requires basic knowledge of coding, it is not a clinician-friendly interface yet. Further development of the toolbox should make this technique more accessible to facilitate individualized patient assessment, as well as population-based research studies by clinicians.

Conclusions

Soft tissue asymmetry is predominately presented in the lower-third of the face in skeletal Class III patients. The lower cheek and nose asymmetry were detected to have more extensive and of a greater magnitude of asymmetry than other facial anatomical regions but with various individual variations. The overall facial asymmetry index and the regional facial asymmetry indices were higher in males and patients with chin deviation. Morphometric techniques and computer intensive analysis have allowed sophisticated quantification and visualization of the pointwise asymmetry on the full face. This is useful to capture subtle yet important asymmetry instead of making linear or angular measurements between designated points on the face defined by traditional cephalometry approaches. Objective and comprehensive asymmetry evaluation is essential for diagnosis and treatment planning that facilities clinicians to create a more symmetrical facial outcome.

Supplementary material

Supplementary material is available at *European Journal of Orthodontics* online.

Funding

This work was supported by Beijing Natural Science Foundation (7192227), Beijing Municipal Science & Technology Commission (Z181100001718112) and National Natural Science Foundation (82001091).

Conflict of interest

None to declare.

Data availability

The datasets used in this study are available from the corresponding author on reasonable request.

References

1. Chen Y-J, Yao C-C, Chang Z-C, Lai H-H, Yeh K-J, Kok S-H. (2019) Characterization of facial asymmetry in skeletal Class III malocclusion and its implications for treatment. *International Journal of Oral and Maxillofacial Surgery*, 48, 1533–1541.
2. Claes P, Walters M, Clement J. (2012) Improved facial outcome assessment using a 3D anthropometric mask. *International Journal of Oral and Maxillofacial Surgery*, 41, 324–330.
3. Lum V, Goonewardene M.S, Mian A, Eastwood P. (2020) Three-dimensional assessment of facial asymmetry using dense correspondence, symmetry, and midline analysis. *American Journal of Orthodontics and Dentofacial Orthopedics*, 158, 1–13.
4. Sforza C, Peretta R, Grandi G, Ferronato G, Ferrario V.F. (2007) Soft tissue facial volumes and shape in skeletal Class III patients before and after orthognathic surgery treatment. *Journal of Plastic, Reconstructive & Aesthetic Surgery*, 60, 130–138.
5. Djordjevic J, Pirttiniemi P, Harila V, Heikkinen T, Toma A.M, Zhurov A.I, Richmond S. (2013) Three-dimensional longitudinal assessment of facial symmetry in adolescents. *European Journal of Orthodontics*, 35, 143–151.
6. Klingenberg, C.P. (2002) Morphometrics and the role of the phenotype in studies of the evolution of developmental mechanisms. *Gene*, 287, 3–10.
7. Ercan I, Ozdemir S.T, Etoz A, Sigirli D, Tubbs R.S, Loukas M, Guney I. (2008) Facial asymmetry in young healthy subjects evaluated by statistical shape analysis. *Journal of Anatomy*, 213, 663–669.
8. Adams D.C, Rohlf F.J, Slice D.E. (2004) Geometric morphometrics: ten years of progress following the 'revolution'. *Italian Journal of Zoology*, 71, 5–16.
9. Huanca Ghislanzoni L, Lione R, Cozza P, Franchi L. (2017) Measuring 3D shape in orthodontics through geometric morphometrics. *Progress in Orthodontics*, 18, 38.
10. Klingenberg C.P, Barluenga M, Meyer A. (2002) Shape analysis of symmetric structures: quantifying variation among individuals and asymmetry. *Evolution*, 56, 1909–1920.
11. Claes P, Walters M, Vandermeulen D, Clement J.G. (2011) Spatially-dense 3D facial asymmetry assessment in both typical and disordered growth. *Journal of Anatomy*, 219, 444–455.
12. Claes P, Walters M, Shriver M.D, Puts D, Gibson G, Clement J, Baynam G, Verbeke G, Vandermeulen D, Suetens P. (2012) Sexual dimorphism in multiple aspects of 3D facial symmetry and asymmetry defined by spatially dense geometric morphometrics. *Journal of Anatomy*, 22, 97–114.
13. Tian K, Li Q, Wang X, Liu X, Wang X, Li Z. (2015) Reproducibility of natural head position in normal Chinese people. *American Journal of Orthodontics and Dentofacial Orthopedics*, 148, 503–510.
14. White J.D, et al. (2019) MeshMonk: open-source large-scale intensive 3D phenotyping. *Scientific Reports*, 9, 6085.
15. Walters M, Claes P, Kakulas E, Clement J.G. (2013) Robust and regional 3D facial asymmetry assessment in hemimandibular hyperplasia and hemimandibular elongation anomalies. *International Journal of Oral and Maxillofacial Surgery*, 42, 36–42
16. Duran G.S, Dindaroğlu F, Kutlu P. (2019) Hard- and soft-tissue symmetry comparison in patients with Class III malocclusion. *American Journal of Orthodontics and Dentofacial Orthopedics*, 155, 509–522.
17. Thiesen G, Gribel B.F, Freitas M.P.M. (2015) Facial asymmetry: a current review. *Dental Press Journal of Orthodontics*, 20, 110–125.
18. Ekrami O, Claes P, White J.D, Zaidi A.A, Shriver M.D, Van D.S. (2018) Measuring asymmetry from high-density 3D surface scans: an application to human faces. *PLoS One*, 13, e0207895.
19. Kim S.J, Baik H.S, Hwang C.J, Yu H.S. (2015) Diagnosis and evaluation of skeletal Class III patients with facial asymmetry for orthognathic surgery using three-dimensional computed tomography. *Seminars in Orthodontics*, 21, 274–282.
20. Severt T.R, Proffit W.R. (1997) The prevalence of facial asymmetry in the dentofacial deformities population at the University of North Carolina.

The International Journal of Adult Orthodontics and Orthognathic Surgery, 12, 171–176.
21. Haraguchi S, Takada K.Y.Y. (2002) Facial asymmetry in subjects with skeletal Class III deformity. *The Angle Orthodontist*, 72, 28–35.
22. Kamata H, Higashihori N, Fukuoka H, Shiga M, Kawamoto T, Moriyama K. (2017) Comprehending the three-dimensional mandibular morphology of facial asymmetry patients with mandibular prognathism. *Progress in Orthodontics*, 18, 43.
23. Goto T.K, Nishida S, Yahagi M, Langenbach G.E.J, Nakamura Y, Tokumori K, Sakai S, Yabuuchi H, Yoshiura K. (2006) Size and orientation of masticatory muscles in patients with mandibular laterognathism. *Journal of Dental Research*, 85, 552–556.
24. Yamashita Y, Nakamura Y, Shimada T, Nomura Y, Hirashita A. (2009) Asymmetry of the lips of orthognathic surgery patients. *American Journal of Orthodontics and Dentofacial Orthopedics*, 136, 559–563.
25. Djordjevic J, Lewis B.M, Donaghy C.E, Zhurov A.I, Knox J, Hunter L, Richmond S. (2014) Facial shape and asymmetry in 5-year-old children with repaired unilateral cleft lip and/or palate: an exploratory study using laser scanning. *European Journal of Orthodontics*, 36, 497–505.
26. Alqattan M, Djordjevic J, Zhurov A.I, Richmond S. (2015) Comparison between landmark and surface-based three-dimensional analyses of facial asymmetry in adults. *European Journal of Orthodontics*, 37, 1–12.
27. Xiong Y, Zhao Y, Yang H, Sun Y, Wang Y. (2016) Comparison between interactive closest point and procrustes analysis for determining the median sagittal plane of three-dimensional facial data. *The Journal of Craniofacial Surgery*, 27, 441–444.
28. Matthews H.S, Burge J.A, Verhelst P.J.R, Politis C, Claes P.D, Penington A.J. (2020) Pitfalls and promise of 3-dimensional image comparison for craniofacial surgical assessment. *Plastic and Reconstructive Surgery-Glob Open*, 8, e2847.